Journal of Materials Chemistry A

Accepted Manuscript

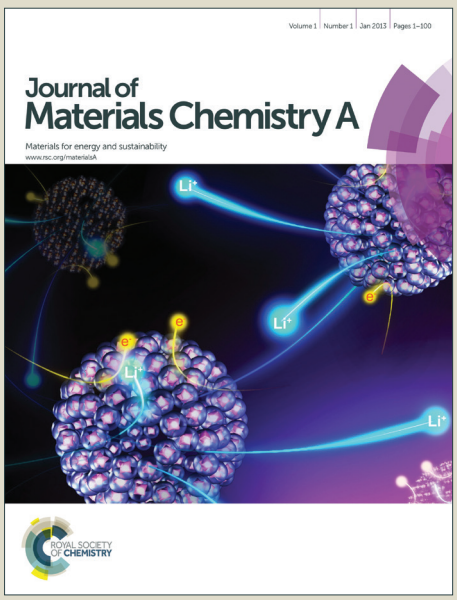

ROYAL SOCIETY OF CHEMISTRY

www.rsc.org/materialsA

Hypercross-linked microporous polymeric ionic liquid membranes: Synthesis, properties and their application in H_2 generation

Amutha Chinnappan, Wook-Jin Chung, Hern Kim*

Energy and Environment Fusion Technology Center, Department of Energy Science and Technology, Myongji University, Yongin, Gyeonggi-do 17058, Republic of Korea.

* Corresponding author. Tel.: +82 31 330 6688; fax: +82 31 336 6336.

E-mail address: hernkim@mju.ac.kr (H. Kim)

Abstract

This work focuses on the hydrogen (H_2) generation from the hydrolysis of sodium borohydride ($NaBH_4$) by using high performance microporous polymeric ionic liquid membranes. Microporous organic polymers are broadly recognized for gas separation and gas storage. In this study, we synthesized hypercross-linked microporous polystyrene (PS) ionic liquid (IL) membranes via in-situ cross-linking by Friedel-Crafts alkylation method. The BET surface area for microporous PS/IL membranes after cross-linking is as high as 852 m^2 g^{-1} compared to non-porous PS/IL membranes before cross-linking (2.7 m^2 g^{-1}) and pure PS membranes (2.5 m^2 g^{-1}). The as-prepared microporous membranes are tested for H_2 generation. The results show that the microporous PS/IL membranes increases the H_2 rate as compared to non-porous membranes. This is due to the dominant factor of hierarchical porosity and high surface area of the membranes. There is no leach or lose of ionic liquid, it is well attached into the cross-linked membranes. The highest rate of H_2 generation (3621 mL H_2 g^{-1} min^{-1}) was observed for 8 wt% of $NaBH_4$ solution, which is comparable to that of noble metal-based catalysts reported in the literature for similar kind of this reaction. The catalyst provided 17290 total turnovers before they are deactivated.

Keywords: ionic liquids, microporous organic polymers, high surface area, H_2 generation, $NaBH_4$

Introduction

Recently, the micro/nano porous materials with astonishingly high surface area have attracted immense attention due to their structures and properties. They have vast potential applications in carbon dioxide separation[1], hydrogen production and storage[2], heterogeneous catalysis[3], and etc. The usefulness of these materials has led scientist to develop a numerous porous materials such as microporous organic polymers (MOPs)[4], metal organic frameworks (MOFs)[5], silica[6], zeolites[7] and carbon based materials.[8] Usually polymer supported ionic liquid membranes are synthesized by mixing polymer and ionic liquid, in which the pores of membranes are filled with ionic liquids. In such kind of membranes, ionic liquids are not chemically attached with polymers, it just trapped inside the pores by a capillary forces. This type of membranes can lose or leach the ionic liquid when it contacts with liquid phase[9]. To tackle the above said problem, special materials should be designed like a non-detachment of ionic liquids from the support. Ionic liquids have been recognized as potential unique materials with more advantageous physical and chemical properties for energy related applications. The salts containing both organic and inorganic charged molecules elicit excellent characteristic at room temperature such as thermally stable, low melting point, low vapor pressure, and non-flammability[10]. More recently, ILs have been using in energy related works due to their potential physicochemical properties. Renewable energy sources have the potential to replace petroleum-derived fuels. At the moment, hydrogen is considered as a potential and promising energy carrier. Hydrogen economy refers to the vision of using hydrogen as a low carbon clean fuel source. Hydrogen is attractive because it produces no emissions at the point of use. However, the hydrogen storage in a safe and more efficient way is still one of the pivotal and challenging problems for hydrogen application. Numerous catalysts[11] have been reported on hydrogen

generation from hydrogen storage materials such as $NaBH_4$, LiH, $LiAlH_4$ and H_3NBH_3. However, they have some drawbacks such as catalyst preparation is complicated and typically entail multiple procedures, utilization of some metal nanoparticles are restricted due to aggregation and low stability. Materials with high surface area provide a potential route to get good dispersion of a catalyst tend to increase the contact area with reactants sufficiently. Therefore, developing new strategies suitable for simple and relatively low-cost materials are necessary. Research reports that synthesis of porous polymers via Friedel-Crafts alkylation reaction is versatile and flexible and allows economical and large-scale production of porous materials. It has become an important method for designing molecules and polymers because this reaction requires relatively mild conditions without any expensive catalyst, but achieves high efficiency. In this paper, we report the use of microporous polymeric ionic liquid membranes for hydrogen generation. These kinds of materials are synthesized in a porous form through chemical cross-linking. First the polystyrene with ionic liquid membranes were prepared, then they have cross-linked via Friedel-Crafts alkylation reaction to produce hypercross-linked porous polymeric ionic liquid membranes. In this approach, formaldehyde dimethyl acetal (FDA) was used as a cross-linker agent, $FeCl_3$ as a catalyst. Hyper cross-linked polystyrene/ionic liquid is a low density and low weight materials with micro/nano-pore structure. The high specific surface area is depending on the higher cross-linking degree of the networks. The typical synthetic pathway is illustrated in Fig. 1a. Fig.1b shows the schematic illustration of Kirkendall effect polymerization for the formation of porous hypercross-linked polystyrene (PS)/ionic liquid (IL) membranes. The formation of porous material is a one-pot, two-step process. The first step involves the synthesis of PS/IL membranes. In the next step, the membranes were added into the mixture of $FeCl_3$ catalyst, Cross-linking agent FDA and 1, 2-dichloroethane solvent. During the

next step, the PS/IL membranes undergo Friedel-Crafts alkylation reaction, to produce a layer of porous materials. Hypercross-linking takes place by the diffusion of atoms or ions through the solid-liquid interface. Due to the faster outward diffusion of atoms or ions, flow of fast-moving vacancies occurred to the proximity of the solid-liquid interface. Therefore, micro/meso pores are formed through vacancies based on Kirkendall effect[12]. The obtained porous PS/IL membranes were tested for hydrogen production from the hydrolysis of sodium borohydride. The porous membranes were generated more hydrogen evolution than non-porous membranes. The typical synthetic pathway of ionic liquid is illustrated in scheme 1.

Experimental Section

Materials

Poly styrene (PS) (average Mw-192,000), $FeCl_3$, $FeCl_2.4H_2O$, dimethoxymethane ie. formaldehyde dimethylacetal (FDA) and 1,2-dichloroethane were purchased from Sigma-Aldrich. Dimethylformamide (DMF) and ethanol were supplied by SHOWA. All the other solvents were of analytical grade and used as received.

Synthesis of 1-allyl-3-methylpyridinium tetrachloroferrate anion

Synthesis of 1-allyl-3-methylpyridinium bromide: To a solution of 3-methyl pyridine (0.054 mol) in ethanol (25 mL) is added to allyl bromide (0.054 mol), and the mixture is refluxed for 24 h. The solvent is removed by rotary evaporation under reduced pressure, and the intermediate (IL-1) is obtained without any purification. It was dried in the vacuum oven at 70 ºC.

Molecular formula (MF) = $C_9H_{12}NBr$; Molecular weight (MW) = 214.1 g/mol, Melting point (MP) = 70.4 ºC; ^{1}H NMR (400 MHz, DMSO-d_6): δ_H (ppm) 9.082 (s, 1H), 8.947-8.962 (d, 1H, J = 6), 8.461-8.481 (d, 1H, J = 8), 8.073 (t, 1H), 6.147 (m, 1 H), 5.423 (2H), 5.281 (2H), 2.467 (s, 3H); ^{13}C NMR (400 MHz, DMSO-d_6): 146.59, 144.74, 142.41, 139.17, 132.17, 127.92, 122.43, 62.27, 39.99, 18.29. LRMS (ESI) Calculated for $C_9H_{12}NBr$ $[M\text{-}Br]^+$ 134.1 found 134.1.

1-allyl-3-methylpyridinium bromide (1 g, 0.004 mol) and $FeCl_2.4H_2O$ (2 g, 0.011 mol) were dissolved in ethanol and stirred at room temperature for four days. After completion of the reaction the solvent was evaporated in rotary evaporator to give the yellowish brown color semi liquid. The obtained product was washed with ethyl acetate several times and dried in vacuum at 60 ºC for 5 h.

MF = $C_9H_{12}Cl_4NFe$; MW = 331.85 g/mol; Thermal decomposition temperature (T_d) = 320 ºC; LRMS (ESI) Calculated for $C_9H_{12}Cl_4NFe$ $[M\text{-}FeCl_4]^+$ 134.1 found 134.1

Synthesis of porous polymeric ionic liquid membranes

The synthetic procedure as follow: The first step is fabrication of polystyrene/ionic liquid membrane followed by cross-linking. PS (Mw 192,000, 40%, w/v) and ionic liquid (3%, w/v) was dissolved in DMF to form polymer solutions. These solutions were placed on a glass substrate and drawn into a membrane using membrane casting knife. Then solvent was allowed to dry for appropriate time. The microporous organic polymer networks were synthesized by Friedel-Crafts alkylation of PS/IL membranes, FDA as a cross-linker, 1,2-dichloroethane as solvent and $FeCl_3$ as a catalyst. The typical procedure is: $FeCl_3$ (0.97 g, 0.006 mol), FDA (0.45 g, 0.006 mol) and 10 ml of 1, 2-dichloroethane was combined and stirred in an ice bath until completely mixed. PS/IL membranes were added to the mixture, and then the mixture was heated

to 80 ºC for 24 h without stirring. The color of the mixture darkens with the time. The resulting membranes were washed with ethyl acetate, and then dried in a vacuum oven at 60 ºC.

Method to test the catalytic activity of porous PS/IL membranes

The catalytic activity of hypercross-linked microporous PS/IL membranes for the hydrolysis of $NaBH_4$ was determined by water displacement method[13]. The reaction flask was placed in a glass reactor equipped with thermostatic bath which maintains the reaction temperature at 30 ± 0.1 ºC. Then, flask filled with water was connected to reaction flask to measure the volume of H_2 gas to be evolved from the reaction. Next, certain amount of catalyst (20 mg) was added into 50 mL of H_2O. Then weighed amount of $NaBH_4$ (158.72 mM) was added into the reaction flask. The reaction was started by closing the reaction flask and volume of H_2 gas evolved was measured by recording the displacement of water level. The amount of accumulated hydrogen was recorded using Balance Talk system. The balance connected with a computer which was installed with the software of 'Balance Talk', can read the balance weight automatically.

Results and discussion

The synthesized ionic liquid (1-allyl-3-methylpyridinium tetrachloroferrate) is semi liquid at room temperature. Thermal decomposition temperature of the IL is 320 ºC, which was studied by thermo gravimetric analysis. The ionic liquid is soluble in water, DMF, DMSO, and insoluble in chloroform, ethyl acetate, ether, THF. The microporous polymeric ionic liquid membranes were synthesized via in-situ cross-linking of non-porous membranes by Friedel-Crafts reaction. The membranes were prepared by mixing of IL and PS in DMF. Then the non-

porous PS/IL membranes were immersed in a mixture of the cross-linking agent FDA, the catalyst $FeCl_3$ and the solvent 1,2-dichloroethane at 80 ºC for 24 h. The cross-linked porous membranes were washed with ethyl acetate and dried in the vacuum at 60 ºC.

Fig. 2 shows the FTIR spectra of non-porous PS membranes, hypercross-linked microporous PS/IL membranes and ionic liquid. As can be seen from Fig. 2 all the important characteristic peaks of PS and IL can be found in the hypercross-linked microporous PS/IL membranes. Especially the aromatic C=C peaks appears at 1601 cm^{-1} and C-H stretching vibration peak appears at 3025 cm^{-1}. The peaks related to C-H bending vibration appear at 1450 and 1503 cm^{-1}. Hypercross-linked microporous membrane have a new band at 1724 cm^{-1} due to C=O stretching vibration. It occurs during the cross-linking process, some of the cross-linker molecules react with aromatic ring by catalyst $FeCl_3$. Moreover ionic liquid characteristic peaks at 3068, 1631, 1503, 1439, 1199, 680 cm^{-1} can also be found in the hypercross-linked membrane. Therefore, these results demonstrate that ionic liquid attached hypercross-linked porous polymeric membrane successfully prepared by Friedel-Crafts alkylation reaction.

Scanning electron microscopy and transmission electron microscopy were used to scrutinize the morphology and nanostructure of the membranes. Fig. 3a represents the non-porous pure PS membranes and Fig. 3b presents PS/IL membranes before cross-linking. These two membranes show non-porous and dense surface. From the figure (Fig. 3a,b), we can clearly see that there is no micro/macroporous core on the membrane surface. Fig. 3 (c, d) shows the porous PS/IL membrane cross-linked for 6 h and 12 h. As can be seen from these images some pores are formed. However after 24 h cross-linking there was a drastic change on the membrane surface. The non-porous structure transferred to porous. The low and higher magnification of SEM and high resolution of TEM images (Fig. 3e, f, h, i) reveal the honeycomb structure with

hierarchical porosity consist of micro/nanoporous core on the membrane surface. The cross-sectional SEM images (Fig. 3g) clearly show that pores are not only on the surface, which run from the top surface into the underlying microporous layer. TEM images confirm that the porosity is uniformly distributed throughout the interior of the membrane and also a large number of nano pores with mean pore diameter of 2.2 nm can be observed. SEM-EDX spectrum of the hypercross-linked microporous PS/IL membranes was given in Fig. 3j, shows that the main elements C, Fe and Cl are detected. This implies that the ionic liquid containing teteachloroferrate anion is present within the cross-linked PS membranes.

The porous properties of the membranes were analyzed by nitrogen adsorption isotherms at 77 K on a BELSORP-min II analyzer. MOPs were degassed at 60 ºC for 2 h under conditions of dynamic vacuum before analysis. The specific surface areas for N_2 were calculated using the BET model over a relative pressure (P/P_0) range of 0-0.5. Total pore volumes were calculated from the uptake at a relative pressure of 0.990. Fig. 4 shows the N_2 sorption isotherm of (a) pure PS membrane; (b) hypercross-linked PS/IL membrane before cross-linking; after cross-linking (c) 6 h, (d) 12 h, (e) 24 h. Hypercross-linked PS/IL membrane after cross-linking showed a sharp uptake at low relative pressures and a gradually increasing uptake at higher relative pressures with time constants, indicating that these materials contained pores. Table 1 summarizes the characterization data such as surface area, pore volume and mean pore diameter. The BET surface area for porous PS/IL membranes after cross-linking was as high as 852 $m^2 g^{-1}$ compared to non-porous PS/IL membranes before cross-linking (2.7 $m^2 g^{-1}$) and pure PS membranes (2.5 $m^2 g^{-1}$). The average pore diameter of hypercross-linked microporous PS/IL membranes was 2.2 nm. The surface area of porous PS/IL membranes was higher than the similar kind of material reported in the literature[4b] (Porous PS membrane range from 260 to 792 $m^2 g^{-1}$). Although the

support is same for both materials, in the present study the synthetic procedure was slightly modified by incorporating ionic liquid into PS membranes. The high surface area of porous PS/IL membranes confirms that the ionic liquid incorporate into PS and hyper cross-linked was very successful.

The porous polymeric membranes structure can easily fine tuned by adjusting cross-linking time. Fig.3 (c, d, e, f) shows the top view SEM images of porous membranes with different cross-linking time. We have performed the experiments under identical conditions but with different cross-linking times of 6, 12, 24 h. SEM images and BET analysis reveal that surface area of the membranes depend on the cross-linking time. There is no pores are formed before 6 h cross-linking times, dense surface was only observed. Increasing the cross-linking time from 6 to 24 h produced micro, meso and macro pores across the surface of the membrane. But micro pores are observed predominately. The surface area increases from 54.5 to 852 m^2 g-1 with the increase in cross-linking time. Pore volume also varied from 0.0282 to 0.4745 cm^3 g^{-1}. The results are listed in Table 1. These data indicates that adjusting the cross-linking time we can easily control the surface area, pore volume and flexibility of the polymeric membrane. Moreover we have checked the cross-linker FDA concentration also from 0.006 mol to 0.03 mol. But there was no significant change in the surface area.

The catalytic activity of the as-synthesized hypercross-linked microporous PS/IL membranes for $NaBH_4$ hydrolysis was scrutinized at 30 ± 0.1 ºC. The rate of hydrogen production increases with increase the amount of catalyst. In a series of experiments, the catalytic activity of PS membranes with a various loading of ionic liquid (1 wt.%, 2 wt.%, 3 wt.%) were tested in the hydrolysis of $NaBH_4$. The best catalytic activity was achieved by 3 wt.% of IL loaded PS membranes. For all the tests reported hereafter, hypercross-linked

microporous PS membranes containing 3 wt.% of IL was used. The self hydrolysis of $NaBH_4$ without catalyst or only the support PS membranes was negligible. The rate of hydrogen generation astonishingly increased when hypercross-linked microporous PS/IL membranes were introduced into the $NaBH_4/H_2O$ system. This indicates that the IL successfully incorporated into the hypercross-linked microporous PS membranes. To support this point, we have performed another reaction with same experimental conditions by using non-porous PS/IL membranes before cross-linking. As shown in Fig. 5 both porous and non-porous PS/IL membranes demonstrated different catalytic activity. Here to mention that the catalytic active site is ionic liquid, this has attached to the high surface area hypercross-linked porous material. Higher rate of hydrogen generation was obtained by porous PS/IL membranes ie 320 mL H_2 g^{-1} in 60 min, where as non-porous PS/IL membranes gave only 130 mL H_2 g^{-1} min^{-1}. This value is more than two times lower than the porous PS/IL membranes. This is highlighting the dominant factor of hierarchical porosity and high surface area of the membranes. The higher catalytic activity can be attributed to structural characteristics of ionic liquid (which has both organic and inorganic ions) and porous PS membranes. The IL is well attached into hypercross-linked microporous PS membranes. This is preventing the detachment of IL from the support. That's the reason high porosity and high surface area hypercross-linked PS/IL membranes exhibited higher catalytic activity toward $NaBH_4$ hydrolysis compared to non-porous PS/IL membranes.

The effect of $NaBH_4$ concentration on the hydrogen generation rate for the hypercross-linked porous PS/IL membranes catalyzed $NaBH_4$ hydrolysis was also examined by changing the initial concentration of $NaBH_4$ and keep the other reaction conditions constant. Fig. 6a shows the plot of volume of hydrogen generation versus time for different concentration of $NaBH_4$ in the range of 2-8 wt%. As manifested in Fig. 6a with the increase in the concentration of $NaBH_4$, the

amount of H_2 evolution was also increased. The highest rate of H_2 generation (3621 mL H_2 g^{-1} min^{-1}) was observed for 8 wt% of $NaBH_4$ at 4th min (Fig. 6b). This shows that a fast H_2 release starts immediately without any difficulties, indicating microporous PS/IL membranes have very effective catalytic active sites. From the graph, we can see that the amount of H_2 produced is dependent on the amount of $NaBH_4$ used. However, the hydrogen rate decreases gradually when $NaBH_4$ concentration is further increased. This may be due to an increase in the pH value of the concentrated solutions with a resulting increase in their stability. Hypercross-linked microporous PS/IL membranes were very effective materials for $NaBH_4$ hydrolysis reaction compared to other catalyst reported for such kind of reactions. For examples: The rate of H_2 was produced by Ni-Ru catalyst was 400 mL H_2 g^{-1} min^{-1} in this case $NaBH_4$ concentration was (10wt%)[14], Co-B catalyst was produced 880 mL H_2 g^{-1} min^{-1} of hydrogen ([$NaBH_4$] = 20wt%)[15], Raney Co gave 267 (mL H_2 g^{-1} min^{-1}) [16], Co-Mn-B catalyst was given 1140 H_2 mL g^{-1} min^{-1} ([NaBH4] = 7wt%)[17]. PtRu-$LiCoO_2$ catalyst was given 2400 mL H_2 g^{-1} min^{-1} hydrogen rate at 25 ºC with 5 wt.% $NaBH_4$ [18]. Transition metal-doped Co-B alloy catalyst such as Co-Ni-B, Co-Fe-B, Co-Mo-B gave the H_2 rate 1175, 1300, 2875 mL H_2 g^{-1} min^{-1} respectively[19]. Poly (N-vinyl-2-pyrrolidone) protected Au/Ni bimetallic nanoparticles exhibited 2597 mL H_2 g^{-1} min^{-1} rate of hydrogen at 30 ºC with 10 wt.% $NaBH_4$[20]. The higher rate of H_2 evolution by hypercross-linked microporous PS/IL membranes can be attributed to the highly porous nature of the materials. Moreover the catalytic active site of ionic liquid also plays an important role, it is cross-linked with porous PS membranes and that rapidly interact with solute into the reaction medium.

Influence of temperature on hydrogen generation rate for $NaBH_4$ hydrolysis was further investigated by porous PS/IL membranes at different temperature from 30 to 50 ºC with the other reaction conditions remain constant. Fig. 7a depicts the plots of the volume of hydrogen

generated versus time for hypercross-linked microporous PS/IL membranes catalyzed $NaBH_4$ hydrolysis. The reaction temperature showed a remarkable effect on the catalytic performance of porous PS/IL for $NaBH_4$ hydrolysis. From the graph, we can see that the amount of H_2 produced is about 319 mL at 30 ºC, however it was gradually increased to 701 mL at 50 ºC. The rate of hydrogen can be assumed to increase almost linearly with the reaction temperature. As an important kinetic parameter, the activation energy for the microporous PS/IL membranes catalyzed $NaBH_4$ hydrolysis were calculated by Arrhenius equation (1)

$$\ln k = \ln A - (E_a/RT)$$

where k is the reaction rate constant (mol min^{-1} g^{-1}). A is the pre-exponential factor, T is absolute temperature (K), E_a is activation energy (kJ mol^{-1}) and R is gas constant (8.314 J K^{-1} mol^{-1}). An Arrhenius plot of ln k (rate constant) versus the reciprocal of absolute temperature (1/T) is shown in Fig. 7b. From the slope of the straight line, the activation energy for the hypercross-linked microporous PS/IL membranes was calculated to be 52.5 kJ mol^{-1}. This value is much lower than other catalysts reported for similar kind of reaction such as Co-B (64.87 kJ mol^{-1})[15], Co-Ni-P/Pd-TiO_2 (57 kJ mol^{-1})[21], Ru/$LiCoO_2$ (68 kJ mol^{-1})[22], Pt/$LiCoO_2$ (70 kJ mol^{-1})[23], Ru/Graphite (61 kJ mol^{-1})[24].

The stability and catalytic life time of the catalyst was examined by cyclic hydrolysis reaction (Fig. 8). The complete conversion of H_2 evolution was achieved within 95 min. Then the catalyst was kept constant and the substrate $NaBH_4$ was fed every time until the H_2 gas slowed down. The catalyst hypercross-linked microporous PS/IL membranes exhibited 17290 total turnover number over 185 min. The reusability studies of the catalyst were carried out. After the first recycle, the hypercross-linked microporous PS/IL membranes were filtered from the reaction mixture. The catalyst was then thoroughly washed with ethyl acetate followed by

distilled water then dried in the vacuum oven. This catalyst was used for another four cycles. From the graph (Fig. 9a), it can be seen that there was not much decrease in H_2 gas evolution up to three cycles. But there is some decrease in the activity, this may be attributed to the increase of metaborate concentration in the solution may block the pores of the membranes. Inorder to confirm this point, we have analyzed N_2 sorption isotherm for recycled hypercross-linked microporous PS/IL membranes. We found 701 m2 g-1 BET surface area of the recycled sample. The results are listed in Table 1. Fig. 9b depicts the N_2 sorption isotherm of recycled hypercross-linked porous PS/IL membranes (24 h). SEM and EDX images (Fig. 9c, d) of recycled hypercross-linked microporous PS/IL membranes show that the catalytic active sites (ionic liquid containing tetrachloroferrate anion) are still present in the material. Ionic liquids are not detached from the support. Moreover the SEM image reveals the porous structure of the membrane was not destroyed even after four recycles.

Conclusions

To date, most of the studies on polymeric ionic liquid membranes were prepared by physical blending methods, in this case ionic liquid can easily lose or leach when it contact with liquid phase. In this paper we presented a simple method to produce hypercross-linked microporous organic polymers. We have synthesized microporous PS/IL membrane via in situ cross-linking of non-porous PS/IL membrane. The catalytic activity of hypercross-linked microporous PS/IL membrane on hydrogen generation by hydrolysis of $NaBH_4$ was examined. There was a huge differences observed between porous and non-porous PS/IL membranes in terms of catalytic activity, this can be due to the nature of the supports and their related properties ie morphology, surface area, chemical nature and porosity. This study clearly reveals

that hypercross-linked microporous PS/IL membranes catalytic activity is more than twice higher than the non-porous PS/IL membranes. Importantly, the rate of hydrogen generation was outstanding in the beginning of the experiment in the range of 1358-1083 mL H_2 min^{-1} g^{-1} at 30 ºC. The highest rate of H_2 generation (3621 mL H_2 g^{-1} min^{-1}) was observed for 8 wt% of $NaBH_4$. They found to be long-lived catalyst and provided 17290 total turnovers before they are deactivated.

Acknowledgements

This study was supported by National Research Foundation of Korea (NRF) – Grants funded by the Ministry of Science, ICT and Future Planning (2014R1A2A2A01004352) and the Ministry of Education (2009-0093816), Republic of Korea.

References

1 D.L. Gin, R.D. Noble, *Science* 2011, **332**, 674-676.

2 J. Germain, J. Hradil, J.M.J. Fre´chet, F. Svec, *Chem. Mater*. 2006, **18**, 4430-4435.

3 (a) X. Du, Y. Sun, B. Tan, Q. Teng, X. Yao, C. Su, W. Wang, *Chem. Commun*. 2010, **46,** 970-972; (b) D. Dang, P. Wu, C. He, Z. Xie, C. Duan, *J. Am. Chem. Soc*. 2010, **132,** 14321-14323.

4 (a) M.P. Tsyurupa, V.A. Davankov, *React. Funct. Polym*. 2006, **66**, 768-779; (b) Z.A. Qiao, S.H. Chai, K. Nelson, Z. Bi, J. Chen, S.M. Mahurin, X. Zhu, S. Dai, *Nature Commun*. 2014, DOI: 10.1038/ncomms4705; (c) R. Dawson, E. Stockel, J.R. Holst, D.J. Adams, A.I. Cooper, *Energy Environ. Sci*. 2011, **4**, 4239-4245.

5 G. Ferey, C. Mellot-Draznieks, C. Serre, F. Millange, J. Dutour, S. Surble, I. Margiolaki, *Science* 2005, **309**, 2040-2042.

6 (a) D.A. Maidenberg, W. Volksen, R.D. Miller, R.H. Dauskardt, *Nature Mater*. 2004, **3**, 464-469; (b) M.P. Singh, R.K. Singh, S. Chandra, Prog. Mater. Sci. 2014, 64, 73-120.

7 H. Guo, G. Zhu, H. Li, X. Zou, X. Yin, W. Yang, S. Qiu, R. Xu, Angew. *Chem. Int. Ed. Engl*. 2006, **45**, 7053-7056.

8 J.K. Holt, H.G. Park, Y. Wang, M. Stadermann, A.B. Artyukhin, C.P. Grigoropoulos, A. Noy, O. Bakajin, *Science* 2006, **312**, 1034-1037.

9 (a) J.C. Jansen, K. Friess, G. Clarizia, J. Schauer, P. Izak, *Macromolecules* 2011, **44,** 39-45; (b) M.A. Malika, M.A. Hashima, F. Nab, *Chem. Eng. J*. 2011, **171**, 242-254.

10 (a) T. Welton, *Chem. Rev*. 1999, **99,** 2071-2083; (b) J.L. Anderson, R. Ding, A. Ellern, D.W. Armstrong, *J. Am. Chem. Soc*. 2005, **127**, 593-604; (c) E. Sebastiao, C. Cook, A. Hu, M. Murugesu, J. Mater. Chem. A, 2014, 2, 8153-8173.

11 (a) J.D. Ocon, T.N. Tuan, Y. Yi, R.L. de Leon, J.K. Lee, J. Lee, *J. Power Sources* 2013, **243**, 444-450; (b) Y. Chen, Y. Shi, X. Liu, Y. Zhang, *Fuel* 2015, **140**, 685-692; (c) Z. Li, H. Li, L. Wang, T. Liu, T. Zhang, G. Wang, G. Xie, *Int. J. Hydrogen Energy* 2014, **39**, 14935-14941; (d) J. Cheng, C. Xiang, Y. Zou, H. Chu, S. Qiu, H. Zhang, L. Sun, F. Xu, *Ceram. Int*. 2015, **41**, 899-905; (e) A.H. Reshak, *Int. J. Hydrogen Energy* 2013, **38**, 11946-11954; (f) J. Fu, M. Tegel, B. Kieback, L. Rontzsch, *Int. J. Hydrogen Energy* 2014, **39,** 16362-16371; (g) S. Akbayrak, S. Tanyıldızı, I. Morkan, S. O¨ zkar, *Int. J. Hydrogen Energy* 2014, **39**, 9628-9637.

12 W. Wang, M. Dahl, Y. Yin, *Chem. Mater*. 2013, **25**, 1179-1189.

13 (a) Y. Chen, H. Kim. *Fuel Proc. Technol*. 2008, **89,** 966-972; (b) A. Chinnappan, H. Kim, C. Baskar, I.T. Hwang, *Int. J Hydrogen Energy* 2012, **37**, 10240-10248.

14 C.H. Liu, B.H. Chen, C.L. Hsueh, J.R. Ku, M.S. Jeng, F. Tsau, *Int. J. Hydrogen Energy* 2009, **34,** 2153-2163.

15 S.U. Jeong, R.K. Kim, E.A. Cho, H.-J. Kim, S.-W. Nam, I.-H. Oh, S.-A. Hong, S.H. Kim, *J. Power Sources* 2005, **144,** 129-134.

16 B.H. Liu, Z.P. Li, S. Suda, *J. Alloys Compd*. 2006, **415**, 288-293.

17 X. Yuan, C. Jia, X.L. Ding, Z.F. Ma, *Int. J. Hydrogen Energy* 2012, **37**, 995-1001.

18 W. Ye, H.M. Zhang, D.Y.Xu, L.Ma, B.L. Yi, *J. Power Sources* 2007, **164**, 544-548.

19 N. Patel, R. Fernandes, A. Miotello, *J. Catal*. 2010, **271**, 315-24.

20 X. Wang, S. Sun, Z. Huang, H. Zhang, S. Zhang, *Int. Hydrogen Energy* 2014, **39**, 905-916.

21 M. Rakap, E.E. Kalua, S. Ozkar, *J. Alloys Compd*. 2011, **509**, 7016-7021.

22 Z. Liu, B. Guo, S.H. Chan, E.H. Tang, L. Hong, *J. Power Sources* 2008, **176**, 306-311.

23 Y. Kojima, K. Suzuki, K. Fukumoto, M. Sasaki, T. Yamamoto, Y. Kawai, H. Hayashi, *Int. J. Hydrogen Energy* 2002, **27**, 1029-1034.

24 Y. Liang, H.B. Dai, L.P. Ma, P. Wang, H.M. Cheng, *Int. J. Hydrogen Energy* 2010, **35**, 3023-3028.

Figure captions

Scheme 1. Synthesis of 1-allyl-3methylpyridinium tetrachloroferrate anion

Table 1. Porosity of the membranes

Fig. 1. (a) Synthesis of porous polymeric ionic liquid membranes, (b) Kirkendall effect polymerization.

Fig. 2. FTIR spectra of (a) non-porous PS membranes (b) hypercross-linked porous PS/IL membranes and (c) IL.

Fig. 3. SEM images of (a) non-porous PS membranes; (b) PS/IL membrane before cross-linking; Porous PS/IL membranes after cross-linking (c) 6 h, (d) 12 h, (e, f) 24 h, (g) cross sectional SEM image of the porous PS/IL membrane cross-linked for 24 h; TEM images of porous PS/IL cross-linked membranes. Scale bar (h) 50 nm, and (i) 10 nm; (j) EDX image of Porous PS/IL membranes after cross-linking (24 h).

Fig. 4 N_2 sorption isotherm of (a) pure PS membrane; (b) hypercross-linked PS/IL membrane before cross-linking; after cross-linking (c) 6 h, (d) 12 h, (e) 24 h.

Fig. 5. Volume of H_2 versus time plots for the hydrolysis of 50 mL of 158.72 mM $NaBH_4$ catalyzed by non-porous and hypercross-linked porous PS/IL membranes (20 mg) at 30 ± 0.1 ºC.

Fig. 6. (a) Volume of H_2 and (b) rate of H_2 versus time plots for the hydrolysis of $NaBH_4$ catalyzed by hypercross-linked porous PS/IL membranes (20 mg) with different concentration of $NaBH_4$ at 30 ± 0.1 ºC.

Fig. 7. (a) Volume of H_2 versus time plots for the hydrolysis of (50 mL, 158.72 mM) $NaBH_4$ catalyzed by hypercross-linked porous PS/IL membranes at different temperatures, (b) Arrhenius Plot.

Fig. 8. Total turnover number (TTON) versus time plots for the hydrolysis of $NaBH_4$ catalyzed by hypercross-linked porous PS/IL membranes at 30 ± 0.1 ºC.

Fig. 9. (a) Plot of the volume of hydrogen (mL) versus subsequent catalytic runs for the hydrolysis of sodium borohydride (50 mL, 158.72 mM $NaBH_4$) catalyzed by hypercross-linked porous PS/IL membranes (20 mg) at 30.0 ± 0.1 °C; (b) N_2 sorption isotherm of recycled hypercross-linked porous PS/IL membranes (24 h); (c, d) SEM and EDX image of recycled hypercross-linked porous PS/IL membranes.

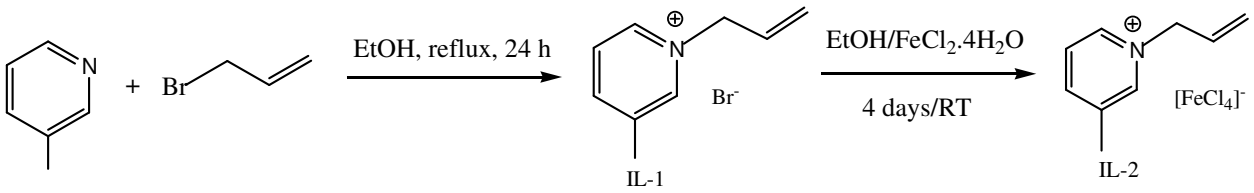

Scheme 1.

Table 1 Porosity of the membranes

S.No	Samples	S_{BET}[a] (m^2/g)	TPV[b] (cm^3/g)	MPD[c] (nm)
1	PS membranes	2.5261	4.3807	6.9369
2	PS/IL membranes before cross-linking	2.7103	0.0047	7.0334
3	Porous PS/IL membranes after cross-linking (6 h)	54.5	0.0282	2.0705
4	Porous PS/IL membranes after cross-linking (12 h)	167	0.0769	1.8416
5	Porous PS/IL membranes after cross-linking (24 h)	852.62	0.4745	2.2261
6	Porous PS/IL membranes (recycled)	701	0.3481	1.9852

[a] Surface area calculated from nitrogen sorption isotherms at 77 k using BET equation; [b] total pore volume; [c] mean pore diameter

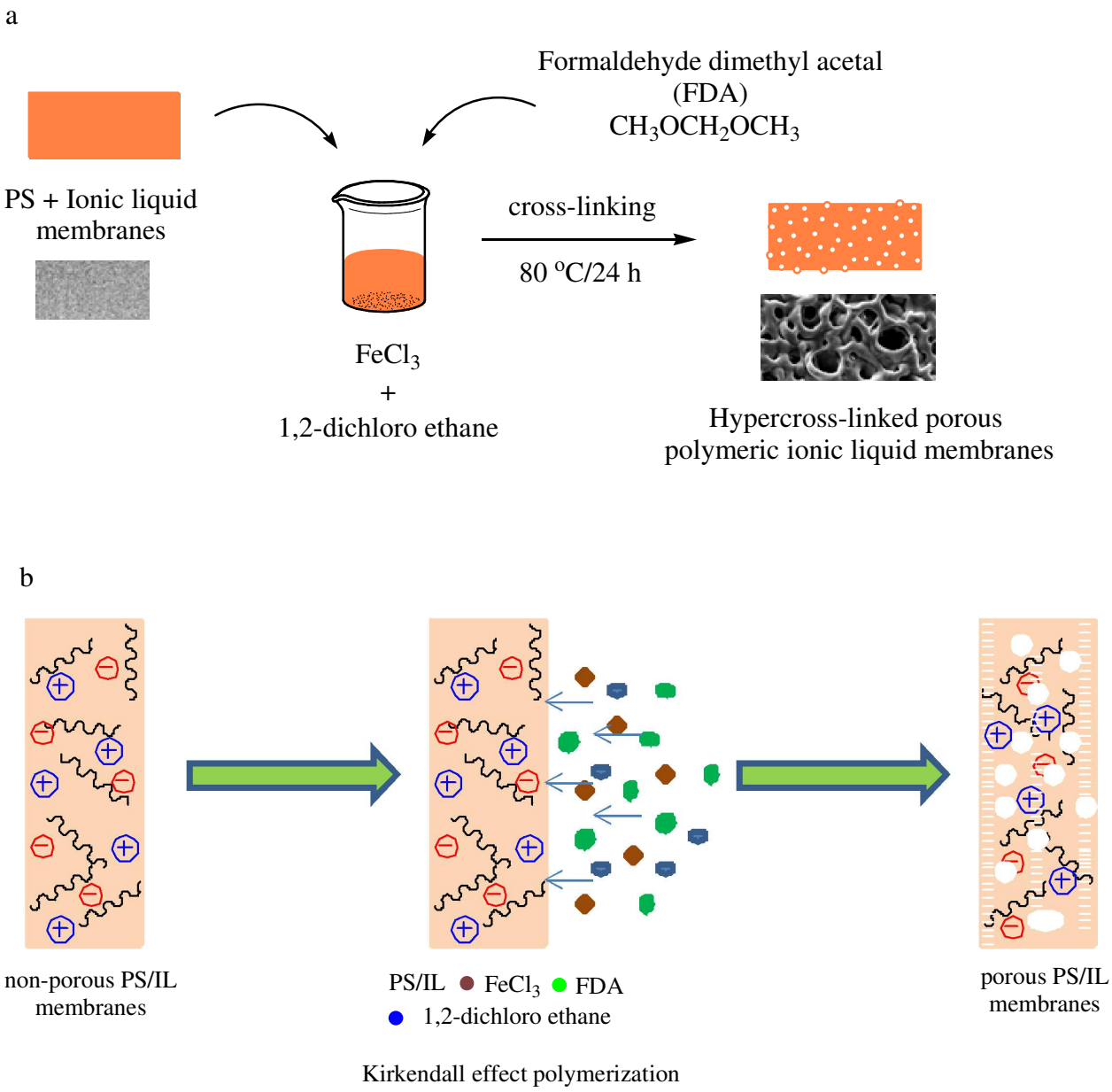

Fig. 1

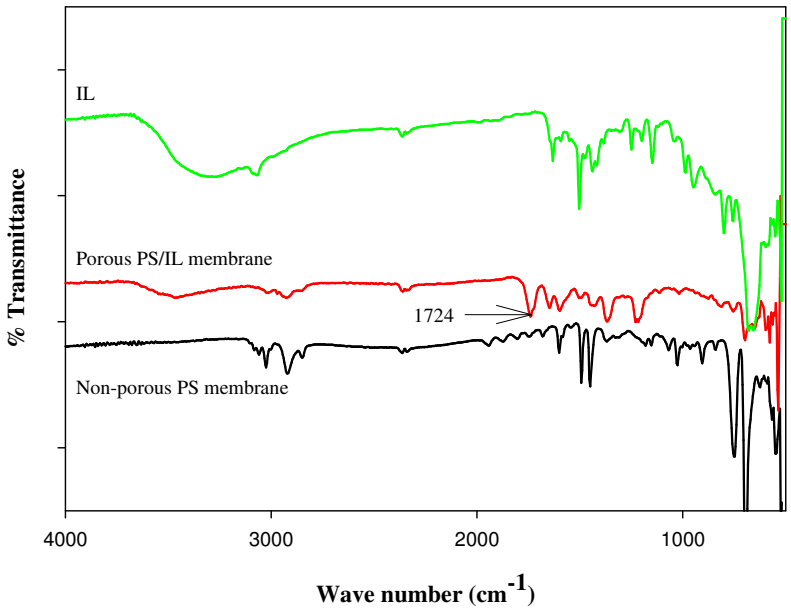

Fig. 2

Graphical Abstract

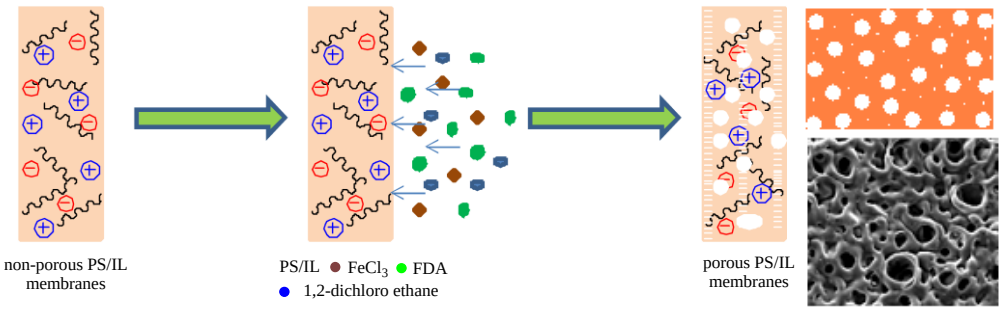

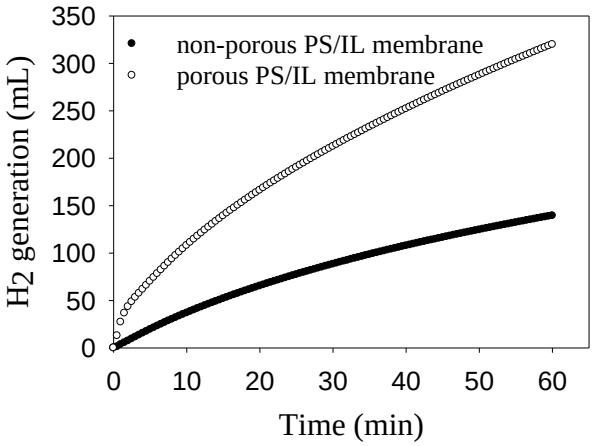

✓Hypercross-linked porous PS/IL membranes
✓High surface area (852 $m^2 g^{-1}$)
✓Mean pore diameter is 2.2 nm

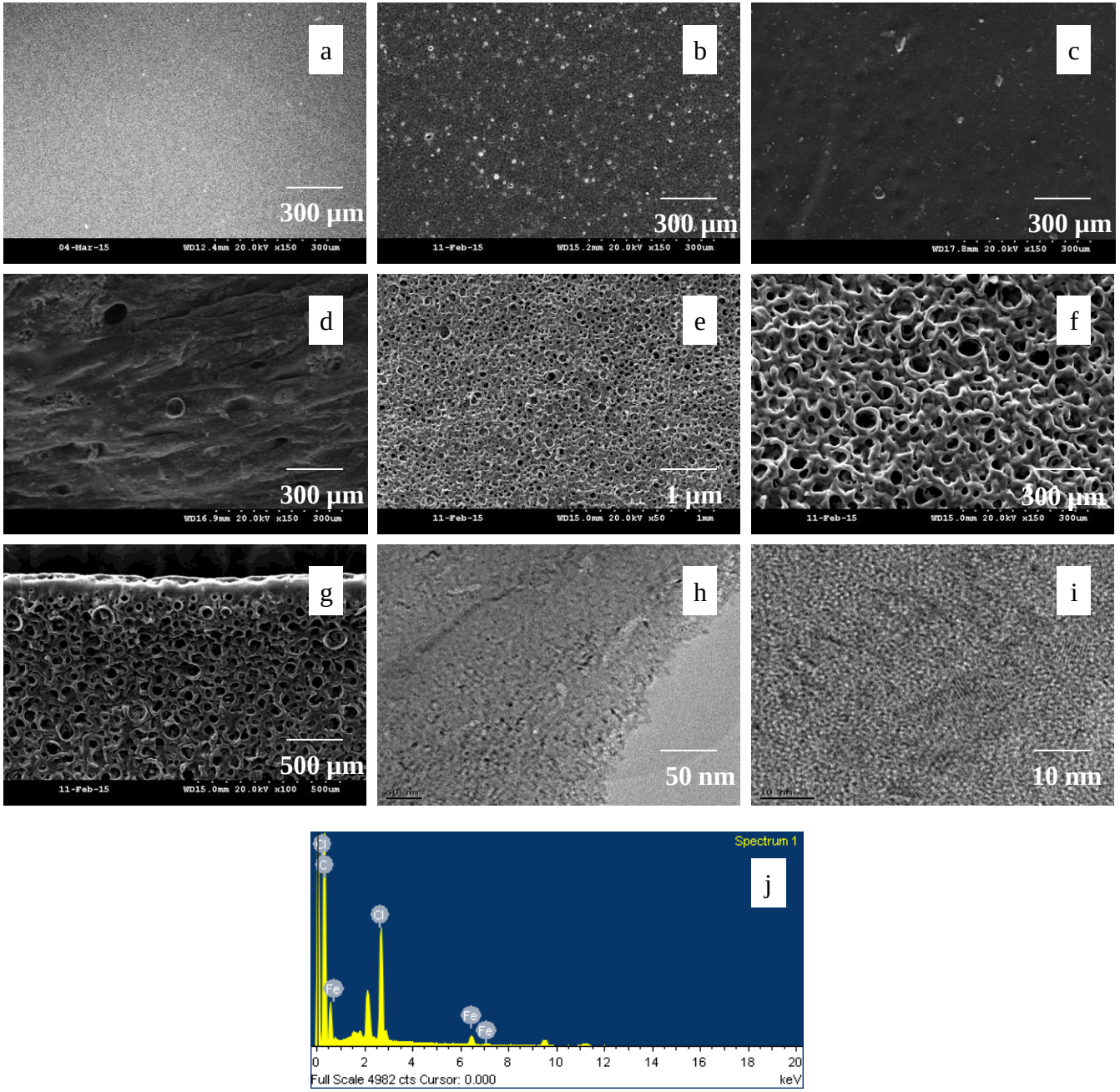

Fig. 3

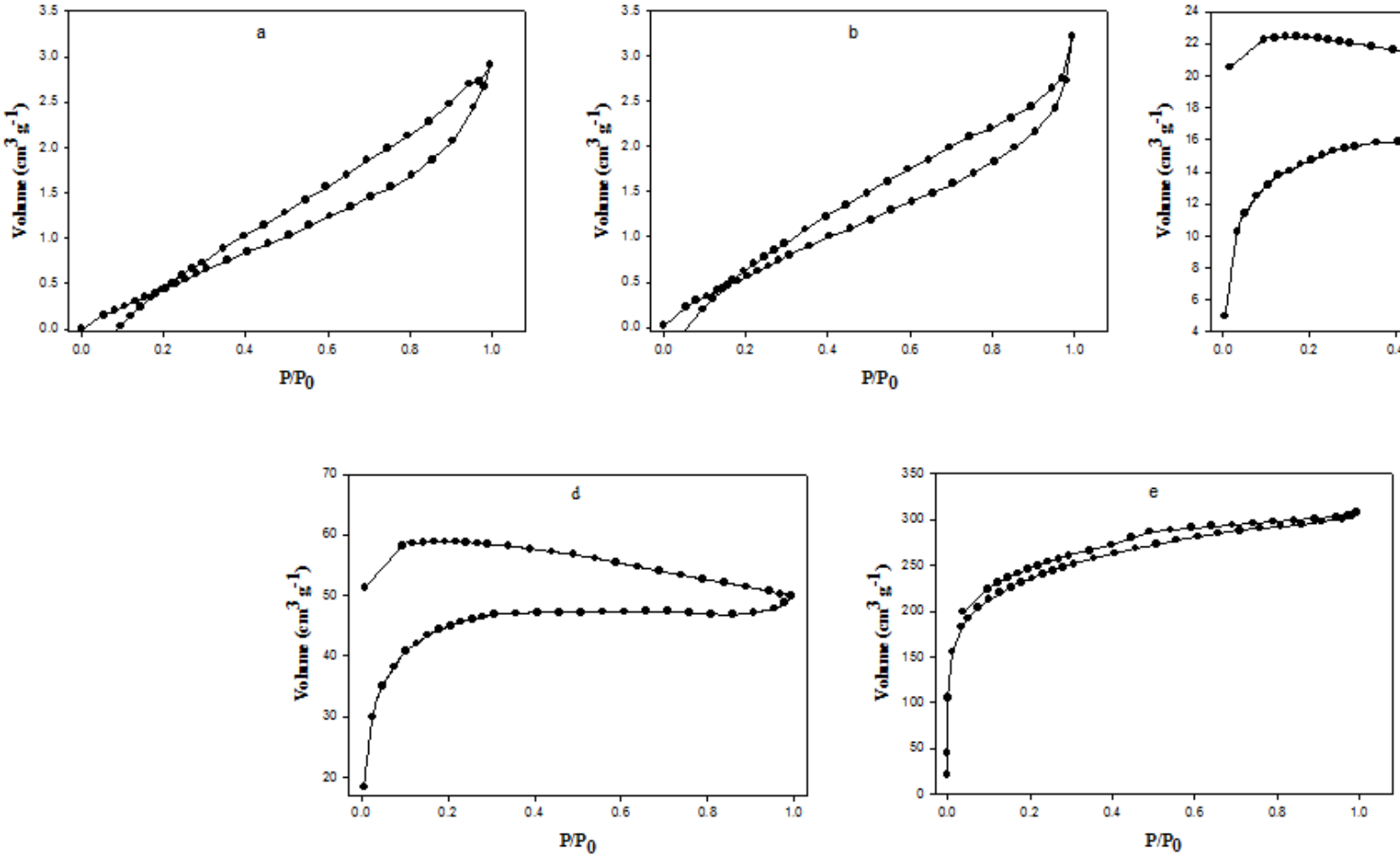

Fig. 4

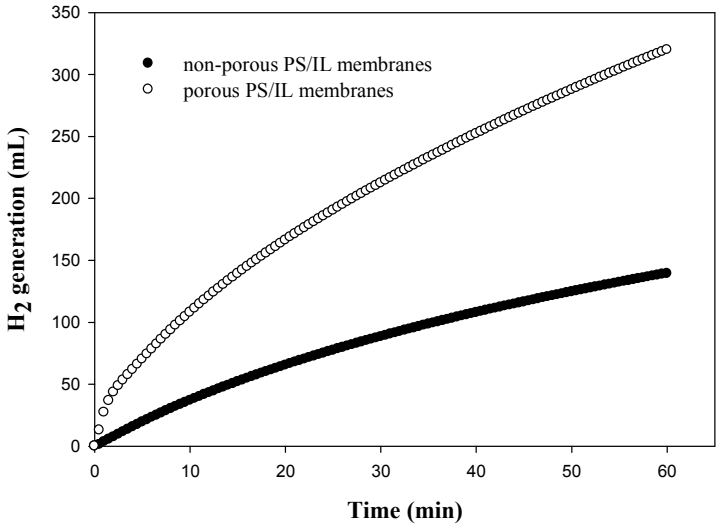

Fig. 5

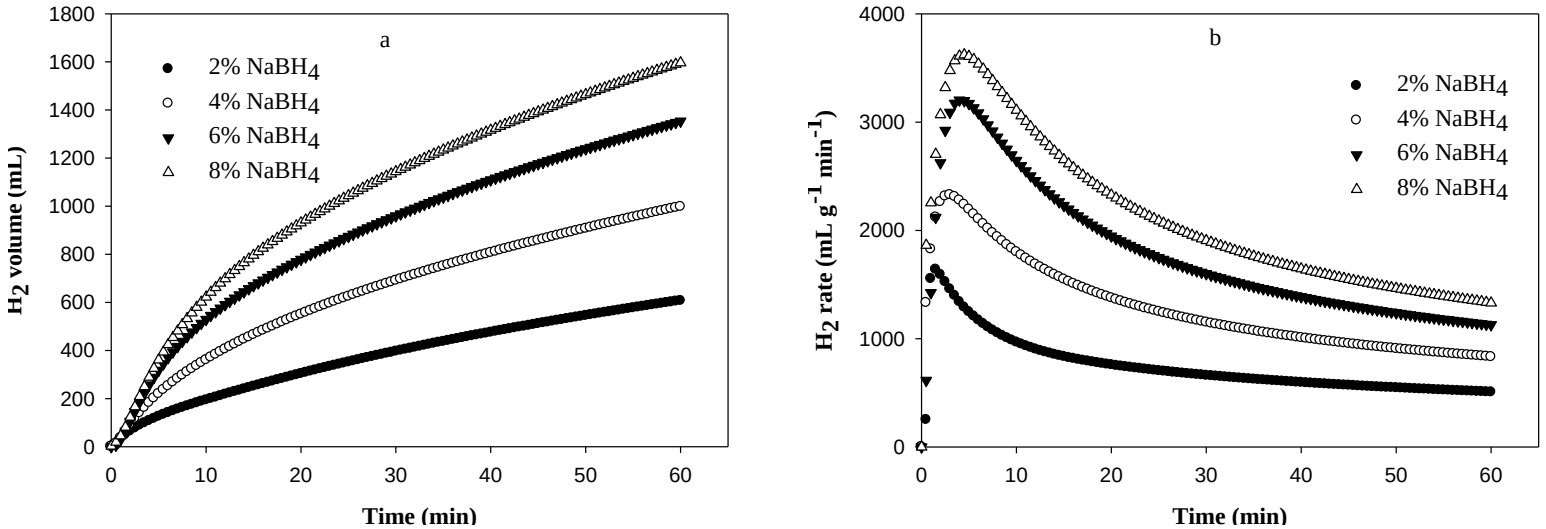

Fig. 6

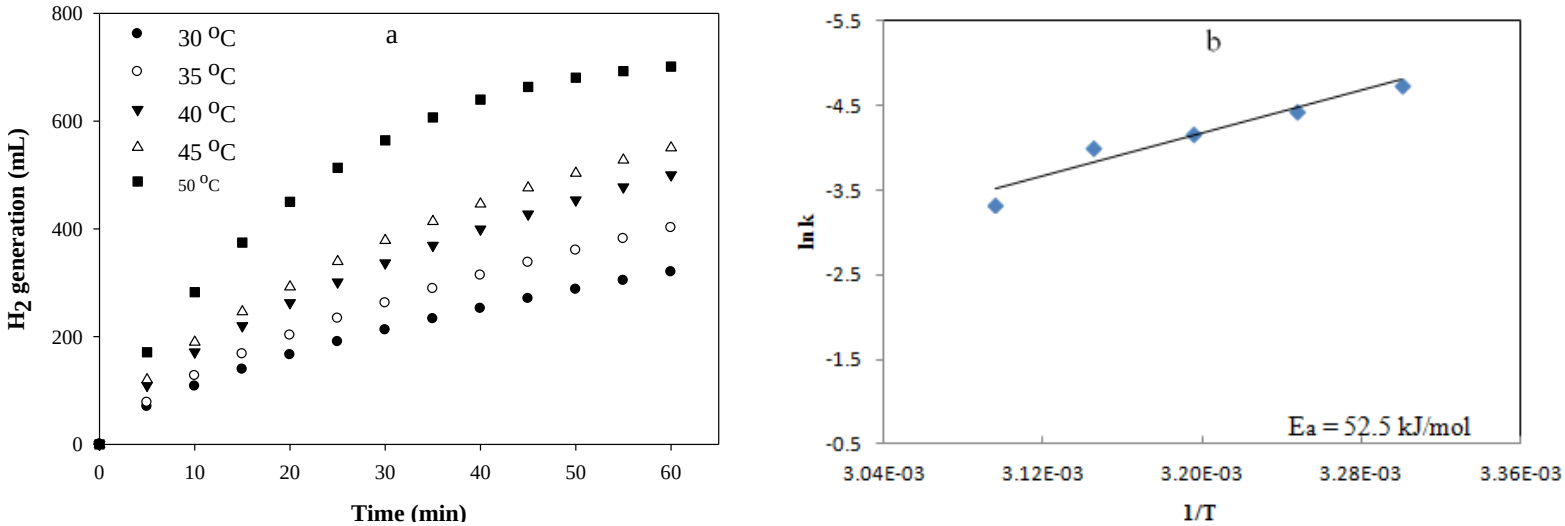

Fig. 7

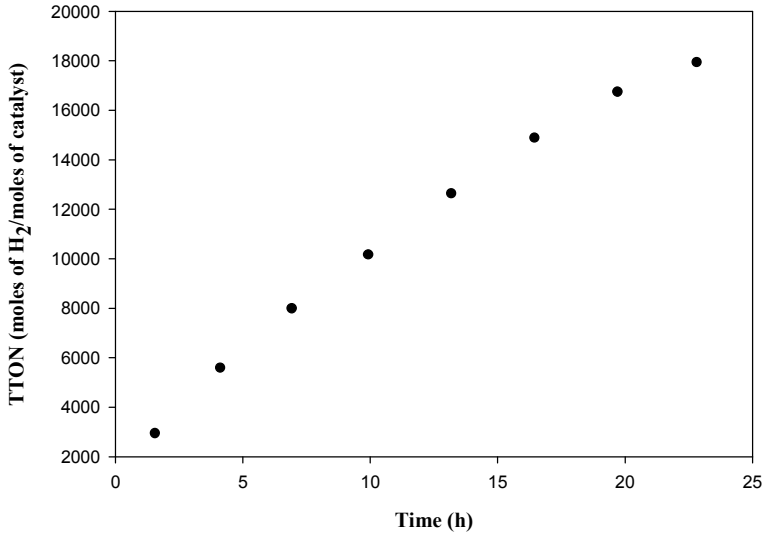

Fig. 8

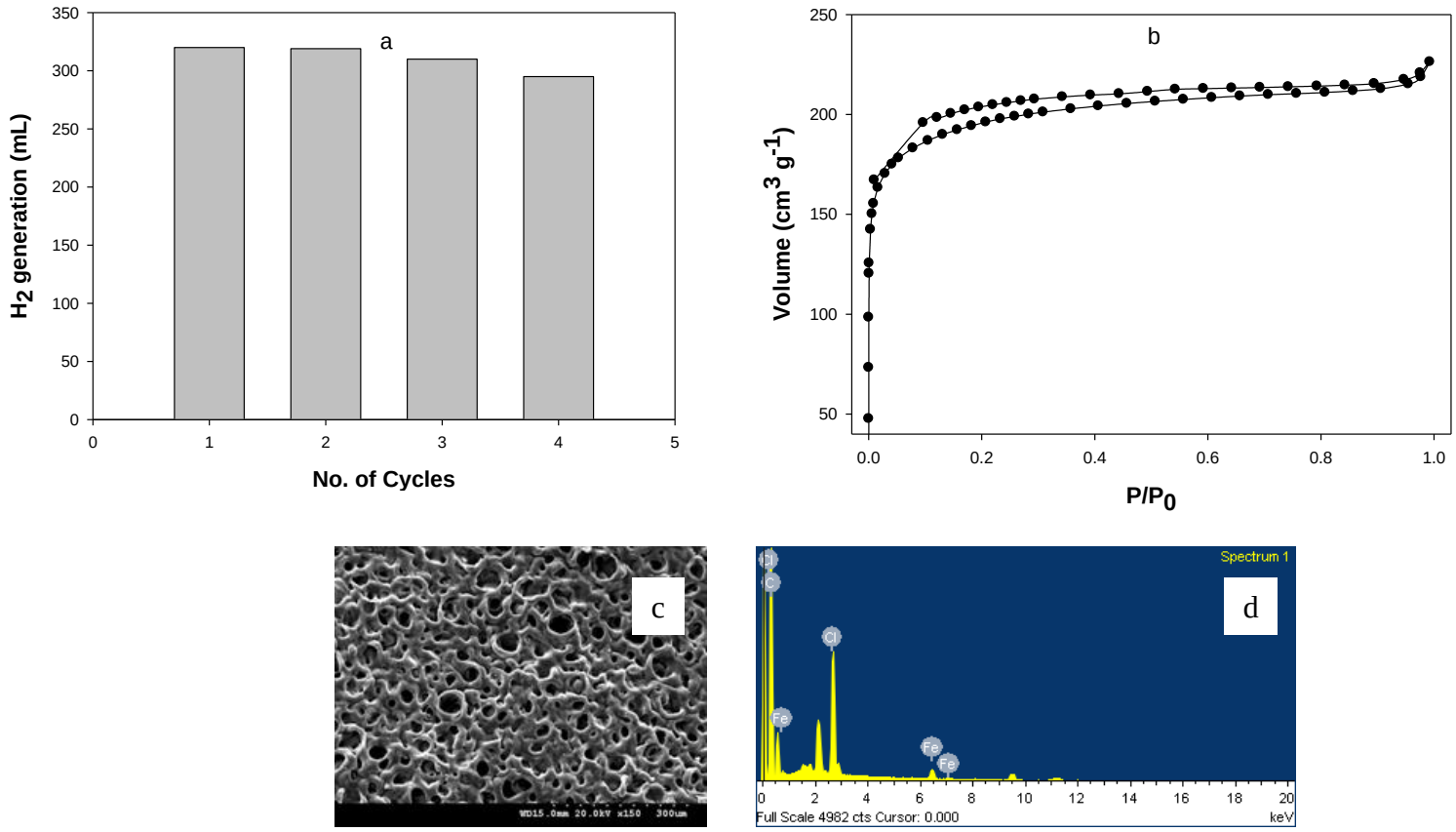

Fig. 9